Two interacting electrons in a one-dimensional parabolic quantum dot: exact numerical diagonalization

2006 J. Phys.: Condens. Matter 18 2623

(http://iopscience.iop.org/0953-8984/18/9/002)

INSTITUTE OF PHYSICS PUBLISHING JOURNAL OF PHYSICS: CONDENSED MATTER

J. Phys.: Condens. Matter **18** (2006) 2623–2633 doi:10.1088/0953-8984/18/9/002

Two interacting electrons in a one-dimensional parabolic quantum dot: exact numerical diagonalization

Orion Ciftja[1] **and M Golam Faruk**[1,2]

[1] Department of Physics, Prairie View A&M University, Prairie View, TX 77446, USA
[2] Department of Electrical Engineering, Prairie View A&M University, Prairie View, TX 77446, USA

Received 23 August 2005
Published 17 February 2006
Online at stacks.iop.org/JPhysCM/18/2623

Abstract

We apply the exact numerical diagonalization technique to study two interacting electrons in a one-dimensional parabolic quantum dot. We consider a modified Coulomb interaction potential between the electrons with a truncation parameter that serves to regularize the behaviour of the bare Coulomb potential in one dimension. We report the dependence of ground and excited state energies for several values of the truncation parameter as the strength of electronic correlations is varied relative to the confinement energy. The similarity of this quantum dot system to the ammonia molecule is pointed out.

During the past years, the application of new and extraordinary experimental tools to nanoscience has generated great interest in some special semiconductor electronic systems, called *quantum dots*. Quantum dots are localized systems generally fabricated by applying a lateral confining potential to a two-dimensional (2D) electron system [1–6]. Quantum dots can contain anything from a single electron to thousands of electrons, and much of their behaviour can be precisely tuned by using standard nanofabrication methods. There is a strong interest in their study both from the technological and theoretical point of view. From the technological point of view, quantum dots offer the potential to build faster electronic devices, such as single-electron transistors. From the theoretical point of view, they represent a unique opportunity to study fundamental quantum phenomena in a tunable atomic-like set-up and this is the reason why, sometimes, they are referred to as *artificial atoms*. Studies of quantum dots even with as few as two electrons pose many challenges, for the simple reason that, sometimes, standard techniques of condensed matter physics, such as Hartree–Fock methods, are not sufficiently accurate. Therefore, an 'exact' quantum mechanical treatment is needed, and inevitably this requires use of numerical methods. Two 'exact' (in the numerical sense) methods have been successfully applied to quantum dots: one is the exact numerical diagonalization technique [7–12], and the other one is the quantum Monte Carlo (QMC) method [13–16].

A quantum dot consisting of two interacting electrons ($N = 2$) in a parabolic confinement potential constitutes the simplest system in which we can study the set-up of electronic correlations. Despite the simplicity, a lot of useful information can be extracted from the study of this small system, since its behaviour is a good qualitative benchmark to understand larger structures.

A particular motivation for the study of such quantum dots is their relevance to the field of quantum computing [17–20], especially after being shown that two-electron quantum dots have the potential to form the basis of scalable qubits [21] in a future quantum computer.

Generally speaking, a quantum dot is associated with confined and strongly correlated electronic systems in 2D. The first pioneering work on such systems is due to Bryant [22] in which the electronic structure of up to $N \leqslant 6$ electrons confined in a 2D infinite rectangular-well potential was calculated. A Coulomb potential screened by the background dielectric constant was chosen as the form of the electron–electron interaction. In particular, the problem of two interacting electrons in a 2D parabolic confinement potential both in the absence and in the presence of a perpendicular magnetic field has previously been studied by using several methods [8, 23–28]. The exact closed-form solution for the problem of two interacting electrons in both uniform magnetic field and external 2D parabolic potential has been recently reported [29]. The problem of two electrons in a three-dimensional (3D) parabolic confinement potential has also been studied [30, 31].

The objective of the present work is to study two interacting electrons in a one-dimensional (1D) parabolic quantum dot by using the exact numerical diagonalization technique. Because of the peculiarities of the bare Coulomb potential in 1D, instead of the bare Coulomb potential, we consider a truncated Coulomb potential of the form

$$V_\delta(|x_1 - x_2|) = \frac{e^2}{\sqrt{|x_1 - x_2|^2 + \delta^2}}, \tag{1}$$

where $-e(e > 0)$ is the electron's charge and δ is the truncation parameter which regularizes the bare Coulomb potential at $|x_1 - x_2| = 0$. At large distances the truncated Coulomb interaction behaves as a bare Coulomb potential. Such a form of the electron–electron potential has been previously considered in a study of up to four interacting electrons in a 1D infinite square-well potential [32], where the truncation parameter is interpreted as a measure of the width of the electron wave function in the transverse direction.

The choice made in equation (1) is motivated by studies of 3D quantum dots with confinement potential of the form $U(\vec{r}) = U_{2D}(x, y) + U_z(z)$, where the parabolic confinement in the third dimension, $U_z(z)$, is weaker than the 2D parabolic confinement, $U_{2D}(x, y)$ and $\vec{r} = (x, y, z)$. When the confinement frequency, ω, in the third dimension is much smaller than the 2D confinement frequency, the two-electron wavefunction can be written as $\Psi(\vec{r}_1, \vec{r}_2) = \Psi_{2D}(x_1, y_1, x_2, y_2)\Psi_z(z_1, z_2)$. After integrating out the 2D coordinates, the effective 1D electron–electron interaction becomes

$$U_{1D}(z_1, z_2) = e^2 \int \mathrm{d}^2 r_1 \int \mathrm{d}^2 r_2 \frac{|\Psi_{2D}(x_1, y_1, x_2, y_2)|^2}{\sqrt{|x_1 - x_2|^2 + |y_1 - y_2|^2 + |z_1 - z_2|^2}}. \tag{2}$$

This expression is of Coulomb form when $|z_1 - z_2| \to \infty$, but does not diverge when $z_1 = z_2$. The non-singular potential in equation (1) is a simple and accurate phenomenological choice that represents such behaviour.

Because the problem under consideration is a 1D problem, without loss of generality, the 1D coordinate is referred to as the x coordinate. Therefore, we write the Hamiltonian describing

two interacting electrons in a 1D parabolic quantum dot as

$$\hat{H} = \sum_{i=1}^{2} \left[\frac{\hat{p}_i^2}{2m} + \frac{m}{2}\,\omega^2\, x_i^2 \right] + V_\delta(|x_1 - x_2|), \tag{3}$$

where $\hat{p}_i$ and x_i are respectively the 1D momentum operator and position of the ith electron, m is the electron's mass, and ω is the angular frequency of the parabolic confining potential. If we introduce the centre-of-mass (CM) and relative motion coordinates:

$$X_{\rm C} = \frac{x_1 + x_2}{2}; \qquad \hat{P}_{\rm C} = \hat{p}_1 + \hat{p}_2; \qquad x = x_1 - x_2; \qquad \hat{p} = \frac{\hat{p}_1 - \hat{p}_2}{2}, \tag{4}$$

the Hamiltonian decouples and can be written as $\hat{H} = \hat{H}_{\rm C} + \hat{H}_{\rm r}$, where $\hat{H}_{\rm C}$ and $\hat{H}_{\rm r}$ are

$$\hat{H}_{\rm C} = \frac{\hat{P}_{\rm C}^2}{2M} + \frac{M}{2}\,\omega^2 X_{\rm C}^2, \tag{5}$$

and

$$\hat{H}_{\rm r} = \frac{\hat{p}^2}{2\mu} + \frac{\mu}{2}\,\omega^2 x^2 + V_\delta(|x|), \tag{6}$$

where $M = 2m$ is the total mass and $\mu = m/2$ is the reduced mass. As a result, the wavefunction for two interacting electrons in a 1D parabolic quantum dot can be written as $\Psi(x_1, x_2) = \Phi_{\rm C}(X_{\rm C})\,\Phi_{\rm r}(x)$, where $\Phi_{\rm C}(X_{\rm C})$ and $\Phi_{\rm r}(x)$ are, respectively, the CM and relative motion wavefunctions. The eigenfunctions and eigenenergies of the CM Hamiltonian are well known:

$$\Phi_{\rm C}(X_{\rm C}) = N_{n_{\rm C}} \exp\left(-\frac{\alpha_{\rm C}^2 X_{\rm C}^2}{2}\right) H_{n_{\rm C}}(\alpha_{\rm C} X_{\rm C}), \tag{7}$$

$$E_{n_{\rm C}} = \hbar\omega\left(n_{\rm C} + \tfrac{1}{2}\right); \qquad n_{\rm C} = 0, 1, \ldots, \tag{8}$$

where $N_{n_{\rm C}} = \sqrt{\frac{\alpha_{\rm C}}{\sqrt{\pi}\,2^{n_{\rm C}} n_{\rm C}!}}$ is a normalization constant, $\alpha_{\rm C} = \sqrt{\frac{M\omega}{\hbar}} = \sqrt{2}\alpha$, where $\alpha = \sqrt{m\omega/\hbar}$ and $H_{n_{\rm C}}(\alpha_{\rm C} X_{\rm C})$ are Hermite polynomials.

Since the truncated Coulomb potential does not affect the CM motion, the problem reduces to the calculation of the eigenenergies and eigenfunctions of the relative motion Hamiltonian. This task is accomplished by using the exact numerical diagonalization method. As basis functions to expand the (unknown) relative motion wavefunction, we use relative motion harmonic oscillator states and write $\Phi_{\rm r}(x) = \sum_{n=0}^{M} c_n \psi_n(x)$, where c_n are (unknown) expansion coefficients and $\psi_n(x) = N_n \exp\left(-\frac{\alpha_{\rm r}^2 x^2}{2}\right) H_n(\alpha_{\rm r} x)$ are the exact eigenstates of the Hamiltonian in equation (6) when $V_\delta(|x|)$ is set to zero, $N_n = \sqrt{\frac{\alpha_{\rm r}}{\sqrt{\pi}\,2^n n!}}$, and $\alpha_{\rm r} = \sqrt{\frac{\mu\omega}{\hbar}} = \alpha/\sqrt{2}$. The minimization of the energy functional, $\langle \hat{H}_{\rm r} \rangle$, with respect to the expansion coefficients gives, as an end result, a matrix eigenvalue–eigenvector problem. The matrix to be diagonalized is of the form $\langle n|\hat{H}_{\rm r}|n'\rangle$, where $n, n' = 0, 1, \ldots M$ and M is the largest quantum number of the harmonic oscillator basis states.

In dimensionless units, the relative motion Hamiltonian matrix elements are

$$h_{nn'} = \frac{\langle n|\hat{H}_{\rm r}|n'\rangle}{(\hbar\omega)} = \left(n + \frac{1}{2}\right)\delta_{nn'} + \frac{\lambda_{\rm r} I_{nn'}}{\sqrt{\pi\, 2^{n+n'} n! n'!}}, \tag{9}$$

where

$$I_{nn'} = \int_{-\infty}^{\infty} {\rm d}t\, {\rm e}^{-t^2} H_n(t) H_{n'}(t) \frac{1}{\sqrt{t^2 + (\alpha_{\rm r}\delta)^2}}, \tag{10}$$

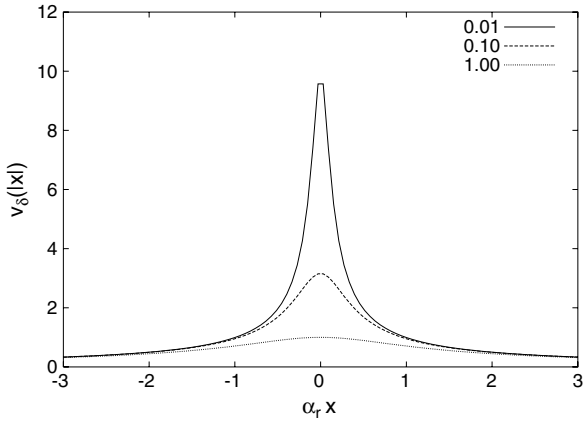

Figure 1. Plot of the dimensionless truncated Coulomb potential, $v_\delta(|x|) = V_\delta(|x|)/(\hbar\omega)$, as a function of $(\alpha_r x)$ for $\lambda_r = 1$ and truncation parameters $(\alpha_r\delta)^2 = 0.01$ (solid line), $(\alpha_r\delta)^2 = 0.10$ (dashed line) and $(\alpha_r\delta)^2 = 1.00$ (dotted line). The parameter $\alpha_r = \sqrt{\frac{\mu\omega}{\hbar}} = \alpha/\sqrt{2}$ has the dimensionality of an inverse length.

and $t = \alpha_r x$ is a dimensionless variable introduced to facilitate the integration of integrals. The dimensionless parameter $\lambda_r = e^2\alpha_r/(\hbar\omega)$ measures the strength of the Coulomb correlation relative to the confinement energy. In dimensionless units, the truncated Coulomb potential has the form

$$v_\delta(|x|) = \frac{V_\delta(|x|)}{\hbar\omega} = \frac{\lambda_r}{\sqrt{(\alpha_r x)^2 + (\alpha_r\delta)^2}}; \qquad \lambda_r = \frac{e^2\alpha_r}{(\hbar\omega)}. \tag{11}$$

In figure 1 we plot the dimensionless truncated Coulomb potential, $v_\delta(|x|)$ for $\lambda_r = 1$ as a function of $(\alpha_r x)$ for three different values: $(\alpha_r\delta)^2 = 0.01, 0.10$ and 1.00.

For any of the above mentioned values of $(\alpha_r\delta)^2$, we select a set of λ_r and build sufficiently large $h_{nn'}$ matrices consisting of $(M+1)\times(M+1)$ elements. We diagonalize the relative motion Hamiltonian using standard numerical methods and the results obtained for finite values of M are extrapolated to the $M \to \infty$ limit. For given values of $(\alpha_r\delta)^2$ and λ_r, the smallest of the energies is identified as the ground state energy of the relative motion Hamiltonian.

It can be proved that, any time that the basis set is enlarged, the eigenvalues of the larger matrix are lower in energy than the corresponding eigenvalues of the smaller matrix. For example, the ground state energy corresponding to the $(M+1)\times(M+1)$ matrix is lower than the ground state energy of the $M \times M$ matrix, which is lower than the ground state energy resulting from a $(M-1)\times(M-1)$ matrix, etc. Since we are using a basis that preserves the linearity of the eigenproblem, the leading error as $M \to \infty$ is proportional to $1/M$. Therefore, in the $M \to \infty$ limit a function of the form $c_0 + c_1/M$ will accurately fit the $\epsilon_r(M)$ energies, obtained for large M. In reality, one has always to deal with a finite basis set (matrix). In such a case, there are two possible ways to extrapolate the results in the $M \to \infty$ limit. When matrix eigenvalues are calculated from matrices that are not very large, a quadratic (in $1/M$) function of the form $c_0 + c_1/M + c_2/M^2$ should be used and will fit the data better. When matrix eigenvalues correspond to large matrices (large basis sets) a linear function of the form $c_0 + c_1/M$ should be used to fit the data (one should not use in this fit the data corresponding to the smaller matrices). Both extrapolation methods should give practically the same result in the $M \to \infty$ limit; however, the first method is less time consuming. The extrapolation procedure for the relative motion energies in the $M \to \infty$ limit is illustrated in figure 2, where we show

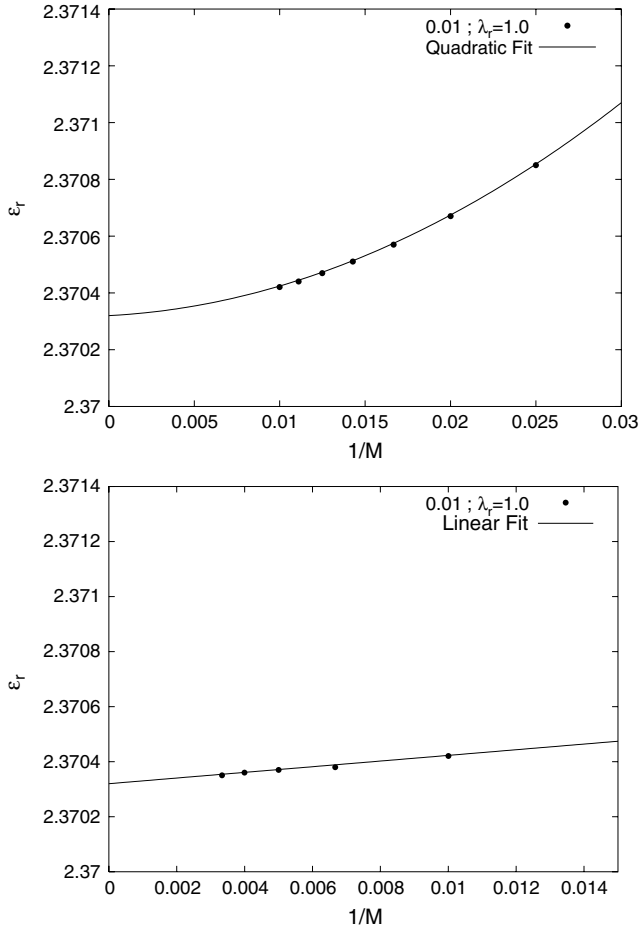

Figure 2. Relative motion ground state energies, ϵ_r, versus $1/M$ for $(\alpha_r\delta)^2 = 0.01$ and $\lambda_r = 1$ obtained from the diagonalization procedure (dots). Top: when the adopted basis set is not very large ($M = 40, 50, \ldots, 100$), a quadratic (in $1/M$) function, $2.370\,32 + 0.003\,143\,02/M + 0.728\,713/M^2$, is the best fit of the diagonalization data (solid line). Bottom: when only large basis sets are considered ($M = 100, \ldots, 300$), a linear (in $1/M$) function, $2.370\,32 + 0.001\,028\,57/M$, is the best fit of the diagonalization data (solid line). Both linear and quadratic extrapolation functions give the same extrapolated value in the $M \to \infty$ limit.

the relative motion ground state energies, ϵ_r corresponding to the system with $(\alpha_r\delta)^2 = 0.01$ and $\lambda_r = 1$ (dots) and the two (top and bottom) fitting functions (solid lines). One can see that both linear and quadratic extrapolation functions give the same extrapolated value in the $M \to \infty$ limit. The same procedure is applied to all other cases.

The smoother the potential, smaller the basis set needed to achieve the desired accuracy. For potentials that are not very smooth (primarily small $\alpha_r\delta$, but to some extent also larger λ_r) a larger value of M is needed to guarantee the same accuracy as for the smoother potential.

In figure 3 we show the ten lowest relative motion energies, $\epsilon_r = \langle \hat{H}_r \rangle/(\hbar\omega)$, for $(\alpha_r\delta)^2 = 0.01$ as a function of λ_r for values of $\lambda_r = 0, 0.5, 1, 1.5$ and 2. The $\lambda_r = 0$ result corresponds to the energy spectrum of an unperturbed 1D harmonic oscillator. Since the height of the barrier at $x = 0$ is $v_\delta(0) = \lambda_r/\sqrt{(\alpha_r\,\delta)^2} = 10\lambda_r$ for $(\alpha_r\,\delta)^2 = 0.01$, some of the excited

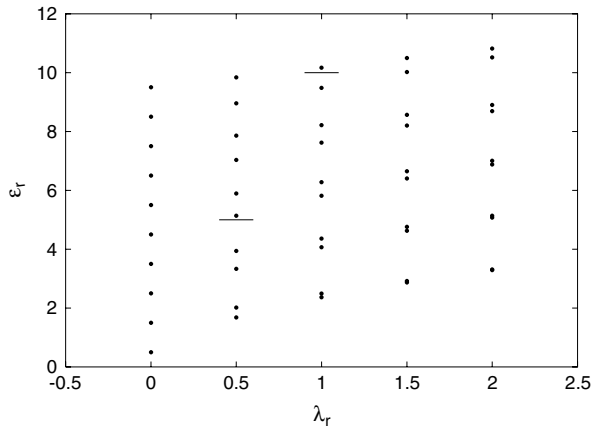

Figure 3. Plot of ten lowest relative motion energies, $\epsilon_r = \langle \hat{H}_r \rangle / (\hbar\omega)$ for $(\alpha_r \delta)^2 = 0.01$ and $\lambda_r = 0, 0.5, 1, 1.5$ and 2. The solid lines represent the height of the barrier, $v_\delta(0)$ for $\lambda_r = 0.5$ and 1.0.

state energies appearing in figure 3 (for instance the energies $\epsilon_r > 5$ for $\lambda_r = 0.5$) correspond to delocalized states.

It is interesting to note that, as the strength of the Coulomb correlation increases, the energy levels converge into doublets. The numerical diagonalization results show that the energies of each doublet become degenerate in the limit of very strong repulsion. This type of behaviour happens for all considered truncation parameters, though it is more pronounced for the smallest truncation parameter $(\alpha_r \delta)^2 = 0.01$, which corresponds to the highest peak of truncated Coulomb potential at the origin. For larger values of the truncation parameter, we need larger values of λ_r to see the doublet creation. In what follows, we focus our attention on the case $(\alpha_r \delta)^2 = 0.01$, where the effects are clearly more visible.

The fact that doublet energies of two different states coincide in the limit of strong repulsion appears puzzling at first given that, in 1D, space symmetric and antisymmetric eigenstates alternate. If $\Psi_{n=0}(x)$ represents the wave function for the lowest energy state of the doublet, it should be space symmetric and, as a result, the wavefunction of the other higher energy state of the doublet, $\Psi_{n=1}(x)$, should be space antisymmetric. However, despite the different symmetry of the states, the diagonalization results show that in the limit of very strong repulsion both have the same energy. This can be explained only if one assumes that, in the limit of very strong repulsion, the symmetric state of each doublet transforms into the mirror reflection of the antisymmetric state of that doublet. Namely, $\Psi_{n=0}(x) \rightarrow |\Psi_{n=1}(x)|$ in the limit of very strong repulsion and same applies to all doublet states. We can intuitively reach the same conclusion if we recall that symmetric states (such as $n = 0$) are nodeless at the origin, but antisymmetric states (such as $n = 1$) have nodes there. Because a very strong truncated Coulomb potential is peaked at $x = x_1 - x_2 = 0$, such a potential will affect the symmetric state much more than the antisymmetric one. The resulting effect would the appearance of a node-like drop of the symmetric wavefunction at $x = x_1 - x_2 = 0$, something resembling the existing node of the antisymmetric state at $x = x_1 - x_2 = 0$. Therefore, in the strong repulsion limit, the symmetric wavefunction of each doublet becomes identical to the absolute value of the antisymmetric wavefunction of that doublet.

The developing node-like drop of the symmetric wavefunction at $x = x_1 - x_2 = 0$ is clearly seen in the diagonalization results for the ground state relative motion wavefunction.

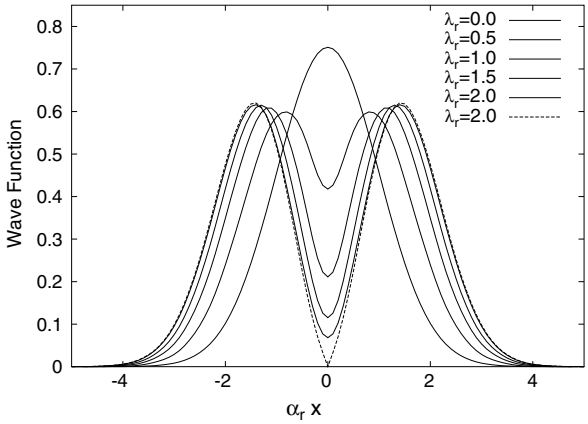

Figure 4. Relative motion ground state wavefunction (full line) for two interacting electrons in a 1D parabolic quantum dot for a truncated Coulomb potential with truncation parameter $(\alpha_r\delta)^2 = 0.01$ and several values of the dimensionless parameter $\lambda_r = e^2\alpha_r/(\hbar\omega)$. The curve (full line) with the largest value at the origin corresponds to $\lambda_r = 0.0$, and in decreasing order the curve (full line) with the smallest value at the origin corresponds to $\lambda_r = 2.0$. The dashed line represents the absolute value of the relative motion first excited state wavefunction for $\lambda_r = 2.0$. The parameter $\alpha_r = \sqrt{\mu\omega/\hbar}$, where μ is the reduced mass, has the dimensionality of an inverse length.

The full lines in figure 4 represent the ground state wavefunction for the relative motion of two interacting electrons in a 1D parabolic quantum dot with a truncation parameter: $(\alpha_r\delta)^2 = 0.01$ and values of $\lambda_r = 0.0, 0.1, 0.3, 0.5, 1.0$, and 2.0. The dashed line represents the absolute value of the first excited state wavefunction for the relative motion when $\lambda_r = 2.0$. It is apparent that, even for $\lambda_r = 2.0$, the ground state relative wavefunction is not much different from the absolute value of the first excited state (with minor differences only for small x). In the $\lambda_r \to \infty$ limit, the two states become identical. As the strength, λ_r, of the Coulomb correlation increases, the ground state wavefunction of the relative motion (that is Gaussian for $\lambda_r = 0.0$; noninteracting electrons) gradually transforms into a two-peaked wavefunction, where the two electrons are separated in opposite sides of a two-well potential that has the finite truncated Coulomb potential as a barrier in the middle at $x = 0$.

The degeneracy between ϵ_0 (ground state) and ϵ_1 (first excited state) as a function of λ_r can be affected by tuning the parameter $\alpha_r\delta$. For larger $\alpha_r\delta$, for instance $(\alpha_r\delta)^2 = 0.1$ versus 0.01, the values of λ_r have to be bigger to see similar doublets. This can be clearly seen by comparing figure 4 with 5, where for the same λ_r the doublet structure is more pronounced for $(\alpha_r\delta)^2 = 0.01$ than for $(\alpha_r\delta)^2 = 0.1$. Obviously, for larger values of $\alpha_r\delta$ the relative coordinate double-well potential (resulting from the parabolic confinement and Coulomb repulsion) is weaker at the centre, therefore a larger Coulomb repulsion is needed to separate the pair of electrons.

The total (dimensionless) energy of the two interacting electrons in the 1D parabolic quantum dot, $\epsilon = \langle\hat{H}\rangle/(\hbar\omega)$, is $\epsilon = \epsilon_r + \epsilon_{CM}$, where $\epsilon_{CM} = \langle\hat{H}_{CM}\rangle/(\hbar\omega) = (n_C + 0.5)$ and $\epsilon_r = \langle\hat{H}_r\rangle/(\hbar\omega)$ is obtained from the diagonalization procedure.

In particular, the sum of CM ground state energy ($\epsilon_{CM} = 0.5$) and relative motion ground state energy gives the exact numerical diagonalization value of the ground state energy for two interacting electrons in a 1D parabolic quantum dot that is shown in table 1 for given values of λ_r (first column) at $(\alpha_r\delta)^2 = 0.01, 0.10$ and 1.00. All reported values are extrapolations of finite diagonalization results in the $M \to \infty$ limit.

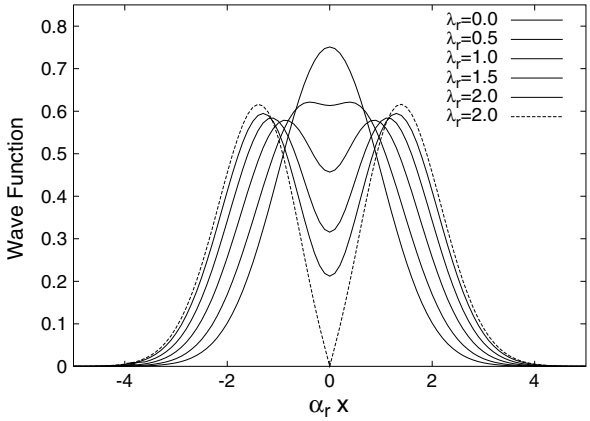

Figure 5. The same as in figure 4, but for $(\alpha_r\delta)^2 = 0.1$.

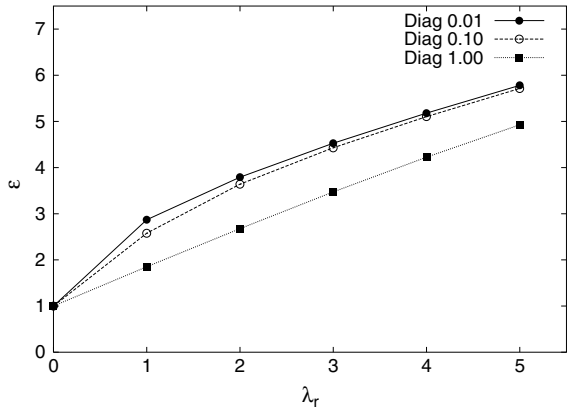

Figure 6. Exact numerical diagonalization (diag) ground state energies, $\epsilon = \langle\hat{H}\rangle/(\hbar\omega)$, for two interacting electrons in a 1D parabolic quantum dot, for values of parameter $\lambda_r = e^2\alpha_r/(\hbar\omega)$ from zero to five. The truncation parameters are respectively $(\alpha_r\delta)^2 = 0.01, 0.10$ and 1.00. The parameter $\alpha_r = \sqrt{\mu\omega/\hbar}$, where μ is the reduced mass, has the dimensionality of an inverse length.

When the total ground state diagonalization energies are compared to first-order perturbation theory results, $\epsilon^{(1)} = 1.0 + \lambda_r I_{00}/\sqrt{\pi}$, it becomes clear that the perturbation theory is reliable only for very small values of λ_r. For larger values, typically $\lambda_r > 1$, first-order perturbation theory is inaccurate. Within the framework of first-order perturbation theory, energies increase linearly with λ_r and as a consequence for $\lambda_r > 1$ they are much higher than the diagonalization values.

In figure 6 we plot the dimensionless ground state energy, $\epsilon = \langle\hat{H}\rangle/(\hbar\omega)$, as a function of the dimensionless Coulomb interaction parameter, $\lambda_r = e^2\alpha_r/(\hbar\omega)$ for values of λ_r ranging from zero (no Coulomb repulsion) up to $\lambda_r = 5$.

If the potential barrier created by the potential shown in figure 1 were of infinite height, the two 'wells' of the resulting relative motion potential would be totally 'disconnected' and the energy spectrum would have consisted of the same set of energy eigenvalues in each well. Thus, each relative motion energy eigenvalue would be doubly degenerate and the relative motion eigenfunctions for a given energy would be linear combinations of $\Psi_R(x)$ and $\Psi_L(x)$,

Table 1. Exact numerical diagonalization ground state energies, $\epsilon = \langle \hat{H} \rangle / (\hbar\omega)$ for two interacting electrons in a 1D parabolic quantum dot in terms of the dimensionless parameter, $\lambda_r = e^2\alpha_r/(\hbar\omega)$ (first column) for a truncated Coulomb potential, with truncation values $(\alpha_r\delta)^2 = 0.01, 0.10$ and 1.00 (second to fourth columns). The parameter $\alpha_r = \sqrt{\mu\omega/\hbar}$, where μ is the reduced mass, has the dimensionality of an inverse length. The statistical uncertainty in the last two digits of energy is shown in parenthesis.

λ_r	$(\alpha_r\delta)^2 = 0.01$	$(\alpha_r\delta)^2 = 0.10$	$(\alpha_r\delta)^2 = 1.00$
0.0	1.000 00	1.000 00	1.000 00
1.0	2.870(32)	2.578(90)	1.850(42)
2.0	3.792(55)	3.640(95)	2.677(59)
3.0	4.527(20)	4.430(56)	3.473(09)
4.0	5.180(14)	5.103(68)	4.226(34)
5.0	5.781(09)	5.713(48)	4.927(18)

which would vanish identically for $x \leqslant 0$ and $x \geqslant 0$, respectively, in the right (R) and left (L) side of the potential barrier.

The space separation of the two electrons leads to the formation of 1D Wigner molecules similar in nature to the Wigner-type arrangement of electrons in a 1D infinite square well in the dilute limit ($\rho = N/L \to 0$) [33].

With a finite barrier, as in the present case, there is coupling between the two 'wells'; as a result the degeneracy is removed, and the relative motion energy levels split into doublets. In what follows, we shall focus our attention on the lowest doublet, which will be treated as a two-level system. Within the Heitler–London framework, one could approximate the two relative motion wavefunctions of the doublet as

$$|\Psi_\pm\rangle = \frac{|1\rangle|2\rangle \pm |2\rangle|1\rangle}{\sqrt{2(1 \pm S^2)}}, \tag{12}$$

where $|1\rangle$ and $|2\rangle$ represent one-particle orbitals centred around a left well at $x = -a$ and around a right well at $x = +a$. The symmetric wavefunction, $|\Psi_+\rangle$, corresponds to the lower energy of the doublet, while the antisymmetric wavefunction, $|\Psi_-\rangle$, corresponds to the higher energy. The left and right orbitals overlap and $S = \langle 1|2\rangle = \langle 2|1\rangle$ denotes their overlap integral. Using ground-state harmonic oscillator orbitals one finds $S = \exp(-\frac{(\alpha d)^2}{4})$, where $d = 2a$ is some mean inter-electron distance. Obviously, the symmetric function corresponds to a spin-singlet state, while the antisymmetric one corresponds to a spin-triplet state. The energy splitting of the doublet, $\Delta E = E_{\text{triplet}} - E_{\text{singlet}}$, is associated with the exchange energy, $J(d) = \Delta E$, which in principle should be highly sensitive to the mean inter-electron distance. The spin dynamics of the system is then described by a Heisenberg spin Hamiltonian of the form

$$\hat{H}_{\text{spin}} = J(d)\vec{S}_1\vec{S}_2, \tag{13}$$

which favours antiparallel spins if $J(d)$ is positive and parallel spins if $J(d)$ is negative. In the following we present a simple idea on how to achieve a high-sensitivity switching of the spin–spin interaction between the electrons, by means of a *static inhomogeneous* electric field. Differently from a static homogeneous electric field, a static inhomogeneous electric field couples to both CM and relative motion, therefore influences the mean separation between the electrons and as a result varies the exchange coupling between the two spins. To have an observable effect, one needs to apply static inhomogeneous electric fields that are non-uniform over distances smaller than or of the same order of magnitude as the size of the 1D parabolic quantum dot. From the experimental point of view, the challenging task is to fabricate a few-electron quantum dot which has a rather large λ_r where the doublets are realized. Let us assume

that, when these conditions are satisfied, the main effect of the static inhomogeneous electric field is to increase the mean distance between the two electrons from d to some value d' ($>d$). Since the overlap and exchange coupling are exponentially sensitive to the inter-electron distance, it is expected that both overlap and exchange coupling will decrease exponentially as the relative distance between the two electrons increases. Clearly, it is the static inhomogeneous electric field that tunes the value of the exchange coupling between the spins. At zero electric field the exchange coupling is 'on', but as soon as a static inhomogeneous electric field is applied the exchange coupling should decrease exponentially to the 'off' state, resulting in a high-sensitivity switching of the spin–spin interactions between a pair of electrons.

In [34] it was suggested that in vertically tunnel-coupled quantum dots the switching of spin–spin interactions can be achieved by using a static homogeneous electric field. Vertically tunnel-coupled quantum dots are essentially 3D structures where two electrons are confined in two different traps ($\omega_1 \neq \omega_2$) and they are spatially separated in the vertical direction. It is clear that, because of the difference in confinement parameters, even a static homogeneous electric field affects the relative motion of the two electrons in that case. Differently from that example, the quantum dot under our consideration has a 1D structure and the two electrons are confined in the same trap, that has frequency ω. Therefore, in our case, we need to use a static inhomogeneous electric field in order to affect the relative motion of the two electrons and consequently change their spin–spin exchange coupling. A uniform static homogeneous electric field couples to the CM motion only, therefore it does not affect the energy splitting of the doublet and cannot be used as a tool to switch spin–spin interactions in our case.

The 1D parabolic quantum dot considered in this work resembles the ammonia (NH_3) molecule. The truncated Coulomb potential between the two electrons in the dot creates the separating barrier, which is similar to the barrier for the N atom created by the Coulomb repulsion between the N nucleus and the three protons of H. Similarly, the 'left' and 'right' electronic states are similar to the 'up' and 'down' states of the vibrational motion of the N atom in the NH_3 molecule. Based on this analogy we speculate on the possibility that a device similar to an ammonia maser [35] may be built out of these parabolic quantum dots.

In conclusion, we considered two interacting electrons in a 1D parabolic quantum dot and solved the problem by using the exact numerical diagonalization technique. We consider a truncated Coulomb potential between the two electrons, where the truncation parameter serves to regularize the behaviour of the bare Coulomb potential in 1D. We report the dependence of ground state and excited state energies as a function of electronic correlations relative to the confinement energy for several values of the truncation parameter. We present a simple idea on how to achieve a high-sensitivity switching of the spin–spin interaction between the electrons, by means of a static inhomogeneous electric field, and point out the similarity of this system to the ammonia molecule.

Acknowledgments

The authors thank Kevin Storr for useful comments. This research was supported by the US DOE (grant No DE-FG52-05NA27036) and by the Office of the Vice-President for Research and Development of Prairie View A&M University through a 2003–2004 Research Enhancement Program grant. One of the authors (MGF) would like to acknowledge the support given through the Title III Program of the US Department of Education.

References

[1] Jacak L, Hawrylak P and Wojs A 1997 *Quantum Dots* (Berlin: Springer)
[2] Ashoori R C 1996 *Nature* **379** 413
[3] Kouwenhoven L P and Marcus C M 1998 *Phys. World* **11** 35

[4] Heitmann D and Kotthaus J P 1993 *Phys. Today* **46** (June) 56
[5] Kastner M A 1993 *Phys. Today* **46** (June) 24
[6] Tarucha S, Austing D G, Honda T, van der Hage R J and Kouwenhoven L P 1996 *Phys. Rev. Lett.* **77** 3613
[7] Maksym P A and Chakraborty T 1990 *Phys. Rev. Lett.* **65** 108
[8] Merkt U, Huser J and Wagner M 1991 *Phys. Rev.* B **43** 7320
[9] Pfannkuche D and Gerhardts R R 1991 *Phys. Rev.* B **44** 13132
[10] MacDonald A H and Johnson M D 1993 *Phys. Rev. Lett.* **70** 3107
[11] Eric Yang S-R, MacDonald A H and Johnson M D 1993 *Phys. Rev. Lett.* **71** 3194
[12] Yannouleas C and Landman U 2000 *Phys. Rev. Lett.* **85** 1726
[13] Maksym P A 1996 *Phys. Rev.* B **53** 10871
[14] Bolton F 1996 *Phys. Rev.* B **54** 4780
[15] Kainz J, Mikhailov S A, Wensauer A and Rössler U 2002 *Phys. Rev.* B **65** 115305
[16] Harju A, Siljamäki S and Nieminen R M 2002 *Phys. Rev.* B **65** 075309
[17] Ekert A and Jozsa R 1996 *Rev. Mod. Phys.* **68** 733
[18] Loss D and DiVincenzo D P 1998 *Phys. Rev.* A **57** 120
[19] DiVincenzo D P 1995 *Phys. Rev.* A **51** 1015
[20] Harju A, Siljamäki S and Nieminen R M 2002 *Phys. Rev. Lett.* **88** 226804
[21] Jefferson J H, Fearn M, Tipton D L J and Spiller T P 2002 *Phys. Rev.* A **66** 042328
[22] Bryant G W 1987 *Phys. Rev. Lett.* **59** 1140
[23] Wagner M, Merkt U and Chaplik A V 1991 *Phys. Rev.* B **43** 7320
[24] Pfannkuche D, Gudmundsson V and Maksym P A 1993 *Phys. Rev.* B **47** 2244
[25] Pfannkuche D, Gerhardts R R, Maksym P A and Gudmundsson V 1993 *Physica* B **189** 6
[26] Harju A, Sverdlov V A, Barbiellini B and Nieminen R M 1998 *Physica* B **255** 145
[27] Ciftja O and Anil Kumar A 2004 *Phys. Rev.* B **70** 205326
[28] Ciftja O and Faruk M G 2005 *Phys. Rev.* B **72** 205334
[29] Kandemir B S 2005 *J. Math. Phys.* **46** 032110
[30] Zhu J-L, Li Z-Q, Yu J-Z, Ohno K and Kawazoe Y 1997 *Phys. Rev.* B **55** 15819
[31] Lamouche G and Fishman G 1998 *J. Phys.: Condens. Matter* **10** 7857
[32] Häusler W and Kramer B 1993 *Phys. Rev.* B **47** 16353
[33] Jauregui K, Häusler W and Kramer B 1993 *Europhys. Lett.* **24** 581
[34] Burkard G, Seelig G and Loss D 2000 *Phys. Rev.* B **62** 2581
[35] Gordon J P, Zeiger H J and Townes C H 1954 *Phys. Rev.* **95** 282
Goldenberg H M, Kleppner D and Ramsey N F 1960 *Phys. Rev. Lett.* **5** 361
Varcoe B T H, Brattke S, Weidinger M and Walther H 2000 *Nature* **403** 743
Chu K R 2004 *Rev. Mod. Phys.* **76** 489